

Highlights

20
14



Energy efficiency oriented



Dielectric Materials and Electrostatics



Foreword

MDE: Dielectric Materials and Electrostatics

The MDE team carries out research on the physical phenomena induced by the electric field in dielectric materials, on the practical applications of these materials, and on the processes involving electrostatic forces. Investigated materials are fluids (liquids and gases) as well as solid materials (especially polymers). These phenomena are mainly: dielectric polarization, injection and transport of electric charges, electric discharges, possibly leading to the breakdown of the insulating materials, and instabilities at liquid interfaces.

The main objectives are the following:

- development of new insulating materials, more respectful of the environment, with enhanced properties, or allowing miniaturization of components and systems;*
- characterize the dielectric materials in representative configurations of their actual use, in particular with the new constraints (i.e. non-sinusoidal and high frequency voltage, high temperatures) generated by the development of new sources (HVDC networks), new uses (automotive, avionics), and new technologies (HV power electronics);*
- assessing the reliability and the lifetime of the insulations by the study of ageing and degradation of the polymer insulating material;*
- design and development of innovative processes based on electrostatic phenomena;*
- production of generic basic knowledge (breakdown mechanisms, conduction).*

Many of the studied phenomena result from inter-correlated mechanisms (electrostatics, chemical, physical), and are often insufficiently understood to allow a predictive modelling. Thus, these researches have a marked multidisciplinary and experimental nature.

Contents

- Experimental and theoretical characterization of the long-range interaction between $\text{He}^*(3s)$ and $\text{He}(1s)$ 5
- Energy harvesting with dielectric elastomers 6
- A thermodynamic model to predict the formation, sizes and mobilities of electron cavities and positively charged ‘snowballs’ in all fluid phases of helium 7
- A New Equation of State for Argon Covering the Fluid Region for Temperatures From the Melting Line to 2300 K at Pressures up to 50 000 MPa 8
- Dielectric characterization of an experimental model of a silica/epoxy interface submitted to a hygrothermal environment 9
- EHD injection of water droplets of controlled micrometric size in dielectric liquids 10
- Infra-Red calorimeter applied to electrical engineering: a new calorimetric device based on thermal radiation for measuring losses in electrical components 11
- Deviations to the Paschen law at distances down to 100 nm: from a gas discharge to a metallic plasma 12
- “Dark” currents in pressurized air and SF6 under HVDC: the crucial role of adsorbed water 13
- Physical and electric properties of various parylene families 14

Directeur de la publication: Nouredine Hadjsaid
 Réalisation : Marie-Thérèse Loubinoux, Mathilde Godon, Service Communication, G2Elab
 Conception couverture: Création d’images, Meylan
 © Photos: Alexis Chezriere, Pierre-Jean Dagnaud, Denis Morel, Sébastien Tillet, G2Elab
 Impression: Service reprographie, Grenoble INP
 Date de publication: 2014

Experimental and theoretical characterization of the long-range interaction between $\text{He}^*(3s)$ and $\text{He}(1s)$

The long-range interaction between $\{1,3\}S \text{He}^*(3s)$ and $1S \text{He}(1s)$ was studied in bulk liquid helium by fluorescence measurements and by combined theoretical electronic structure and bosonic density functional theory calculations. The excited He^* atoms were produced in the liquid by corona discharge with subsequent impact excitation instigated by hot electrons from the discharge. The long-range contribution to the repulsive "hump" near 5 \AA in the $\{1,3\}S \text{He}-1S \text{He}$ potentials was interrogated by monitoring $\text{He}^* \{1,3\}S(3s) \rightarrow \{1,3\}P(2p)$ fluorescence profile characteristics as a function of external pressure between 0.1 and 3.5 MPa.

We have carried out spectroscopic experiments in order to characterize the cryoplasma generated by negative corona discharge in liquid and gaseous helium. Fluorescence spectroscopy can provide detailed information about repulsive upper states when the spectra are recorded systematically as a function of external pressure. Since the surrounding helium density is greater in the liquid phase as compared to helium gas, the liquid phase experiments provide better sensitivity to this interaction. There is a distinct difference between the condensed-phase and gas-phase fluorescence-line-shape behavior as a function of pressure. Thus our experiments detect atomic He^* fluorescence lines, which appear to originate from outside the discharge region. Direct experimental evidence for He^* emitting in the bulk liquid can be obtained by comparing the pressure dependency of the emission line shift for gas versus liquid (see Fig. 1). Due to the low density in the gas phase, the line shift is very small but the spectral broadening is significant due to frequent random collisions with gas-phase He atoms. Conversely, in the liquid, the higher helium density around He^* results in both a large blueshift as well as line broadening. Both the observed singlet and triplet He^* lines exhibit

similar pressure-dependent behavior (apart from quenching) indicating that both species reside in the bulk liquid solvated in bubble states. We have developed an accurate pair potential for $\text{He}^*(3s)\text{-He}$ in both singlet and triplet states using full CI calculations. The accuracy of the potentials was validated by comparing the results from lineshape calculations with experimental spectroscopic data for He^* embedded in liquid at 4.2 K. Bosonic Density Functional Theory simulations and spectroscopic line shape calculations for singlet- and triplet-state $\text{He}^*(3s)$ in liquid helium were carried out to model the experimental observations as a function of external pressure. By analyzing the He^* line shifts as a function of pressure, it was shown that He^* resides inside bubbles, which in turn may be surrounded by a lower-density region created by the excess energy released during the electron-He excitation process. The degree of local heating depends on the He^* preparation method as demonstrated by comparing our 4.2 K data with a similar experiment carried out at 1.8 K. It is demonstrated that the current experimental approach offers a great advantage over the gas-phase measurements by yielding enhanced sampling of the pair potential and thus providing a greater sensitivity for its energetics and curvature

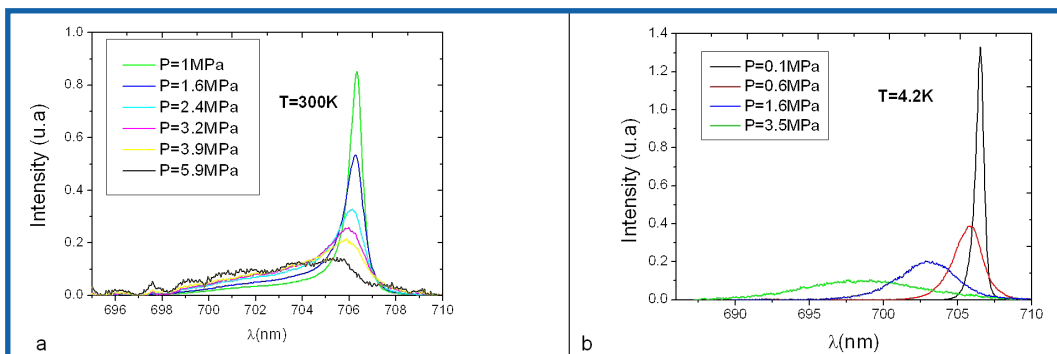


Figure 1 : Variation of experimental profiles of 706 nm line $3s3S-2p3P$ with pressure. Corona discharge at

- a) 300K
- b) 4.2K

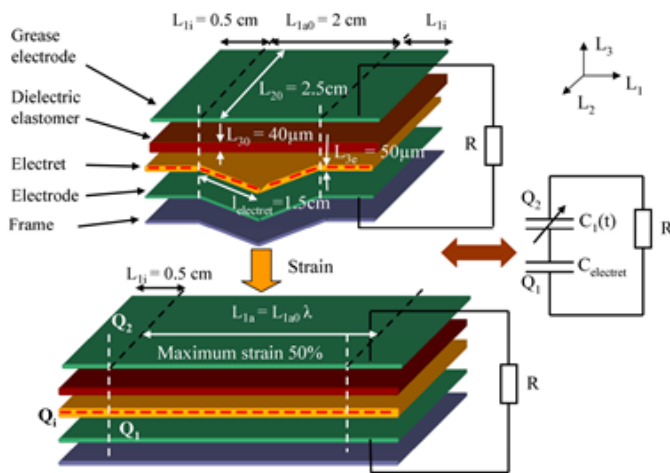
CONTACT

Nelly Bonifaci
nelly.bonifaci@g2elab.grenoble-inp.fr

FURTHER READING

Experimental and theoretical characterization of the long-range interaction between $\text{He}^*(3s)$ and $\text{He}(1s)$
N. Bonifaci, F. Aitken, V.M. Atrazhev, Fiedler S.L., J. Eloranta.
Physical Review A 85 (2012) p 042706

The development of soft electrostatic generators is a promising route for numerous applications. However, the functioning of these generators requires the use of an external high-voltage supply. It has been demonstrated in theory and proven experimentally that this external supply could be advantageously replaced by an electret which is another polymer with inserted space charges inside. This result so allows imagining in a more credible way in the development of generators using this technological approach.



Design of electret-dielectric elastomer generator prototype: at rest and maximal state.

Dielectric elastomer generators offer great potential for soft applications involving fluid or human interactions. These scavengers are light, compliant, have a wide-range of functions and develop an important energy density. Nevertheless, these systems are passive and require an external bias source, namely a high voltage source and complex power circuits. This cumbersome polarization complexes the system in a drastic way and slows down the development of dielectric generators. In order to remove these problems, we propose here new transducers based on the use of an electret coupled with dielectric elastomer, thus avoiding the use of a high external voltage source, and leading to the design of a soft autonomous dielectric generator.

By combining a dielectric model and the electret theory, an electromechanical model was developed to evaluate the capabilities of such a generator. This generator was then produced starting from Teflon™ as electret and silicone Polypower™ as electroactive polymer. A good adequacy between the model and the experiment were obtained. An experimental energy density of 0.55 mJ.g⁻¹ was reached for 50% strain (electret potential -1000 V). Once optimized in its design, such a soft generator could produce energy density up to 1.42 mJ.g⁻¹. An energy density of 4.16 mJ.g⁻¹ is expected with electret potential of -2000 V. These results establish the possibility to the concrete incorporation of flexible and autonomous electrostatic generators for original applications: generators for battery-driven vehicles, generation of energy from waves and wind, generators inside the human body (because biocompatible),...

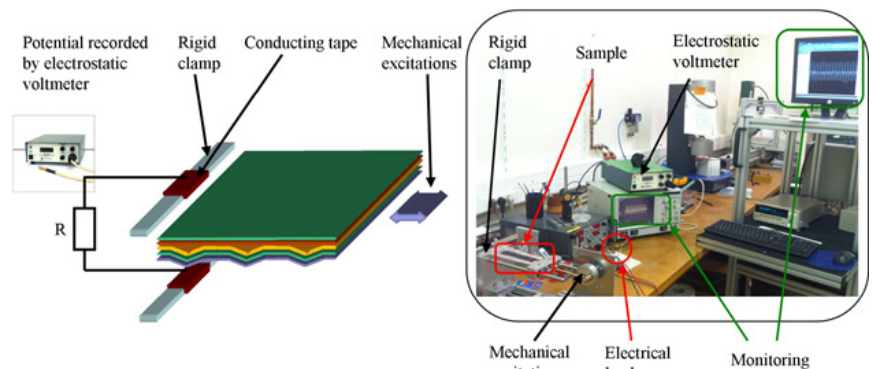
CONTACTS

Ph.D Student
 Claire Jean-Mistral
 Alain Sylvestre
 alain.sylvestre@g2elab.grenoble-inp.fr

FURTHER READING

Advances for dielectric elastomer generators: replacement of high voltage supply by electret
 C. Jean-Mistral, T. Vu-Cong, A. Sylvestre
 Applied Physics Letters, 101, 162901 (5 pp.), 2012.

Electrets substituting external bias voltage in dielectric elastomer generators: application to human motion
 C. Jean-Mistral, T. Vu-Cong, A. Sylvestre
 Smart Materials and Structures, 22, 025012 (13 pp.), 2013.



Dielectric elastomer generator and experimental set-up

A thermodynamic model to predict the formation, sizes and mobilities of electron cavities and positively charged 'snowballs' in all fluid phases of helium

Van der Waals-type thermodynamic state equations are developed for description of mobilities of electron and ion impurities in supercritical and liquid helium. The state equations allow to calculate an effective size of the impurities, i.e. the 'hydrodynamic' radius of electron cavities and of Atkins-snowballs. The mobilities derived from the impurity sizes and the known dynamic viscosities match experimental data with unsurpassed accuracy. This model can be extended to flow at low densities where Knudsen numbers are greater than one by reformulating the Millikan-Cunningham factor to account for size changes of the electron cavities.

Electrons and positive ions are microscopic probes frequently used to explore transport, diffusion and quantum properties of liquid helium. Electrons introduced into liquid helium localise and build large cavities with radii up to 20 Å (at 4.2 K and 1 bar), depending on the pressure. The formation of such voids results from the repulsive interaction between ground state helium atoms and electrons because of the Pauli principle and the very long range van der Waals-like attraction. Positive ions in liquid helium behave the opposite way. In this case, electrostrictive forces between the positive charge and the surrounding polarised helium atoms dominate and attract the helium atoms towards the positive centre. As a consequence a dense, solid-like shell of helium is built, which is why the term 'Atkins-snowball' is often used.

Information of the size that electrons and ions occupy in helium is difficult to obtain in a direct fashion. On the contrary, thanks to the charged nature of electrons and ions, the measurement of their mobility is relatively straightforward to measure using electric fields. The mobility is related to a hydrodynamic radius r via the well known Stokes law for spherical objects

$$\mu_{Stokes} = \frac{e}{6\pi r\eta}$$

and the deduction of the radius requires no other knowledge than the viscosity, η , of the fluid. A number of restrictions nevertheless apply. In particular at low densities where Knudsen number are greater than one the more general Millikan-Cunningham equation must be used instead of Stokes law such that

$$\mu_{MC} = \mu_{Stokes} (1 + \phi)$$

where μ_{MC} is the Millikan-Cunningham mobility and ϕ the Millikan-Cunningham factor.

Finding a coherent description of ion and electron mobility in different density regions, especially the crossover from gas kinetic to Stokes flow is a challenge. An implicit challenge is that ions and electrons in helium are expected to change their structure depending on the density.

We develop thermostatic state equations for electrons and He ions in helium and employ the free volume model to derive the hydrodynamic radius. In general terms, the free volume model relates the size of foreign objects, i.e. solute molecules within a fluid to the size occupied by a free volume unit cell, $(V-b)/N$, using as the first approximation a simple power law between the two. The state equations of P , V and T include parameters which are calibrated using experimentally determined mobilities reported in the literature. The mobilities, μ , are related to the size via the hydrodynamic radius, r , in the Stokes-Einstein equation and by introducing the Millikan-Cunningham factor specifically developed for electrons and ions in helium to account for a large density coverage of our thermodynamic approach, including the gas, supercritical, liquid and superfluid phases (see Figure 1).

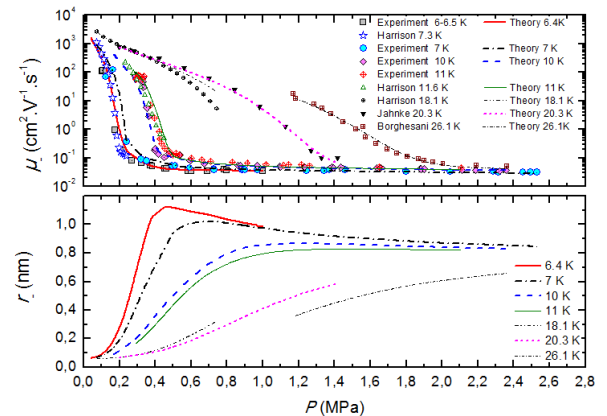


Figure 1: Electron mobility and hydrodynamic radius in the supercritical region of helium. Experimental data of mobilities are taken from Harrison et al. (1973), Jahnke at al. (1971), Borghesani et al. (2002) and ourselves (see the ref. below).

CONTACT

Frédéric Aitken
frederic.aitken@g2elab.grenoble-inp.fr

FURTHER READING

Electron mobility in liquid and supercritical helium measured using corona discharges: a new semi-empirical model for cavity formation

F. Aitken, Z.-L. Li, N. Bonifaci, A. Denat and K. von Haeften
Phys. Chem. Chem. Phys., Vol. 13(2), pp. 719-724, 2011.

A New Equation of State for Argon Covering the Fluid Region for Temperatures From the Melting Line to 2300 K at Pressures up to 50 000 MPa

A new equation of state for argon has been developed, which can be written in the form of a fundamental equation explicit in the reduced Helmholtz free energy. The fundamental equation for the Helmholtz free energy has been derived from the measured quantities $C_v(\rho, T)$ and $P(\rho, T)$. It is valid for the whole fluid region (single-phase and coexistence states) from the melting line to 2300 K at pressures up to 50 000 MPa. The formulation is based on data from NIST and calculated values from the model of Ronchi (1981) for argon.

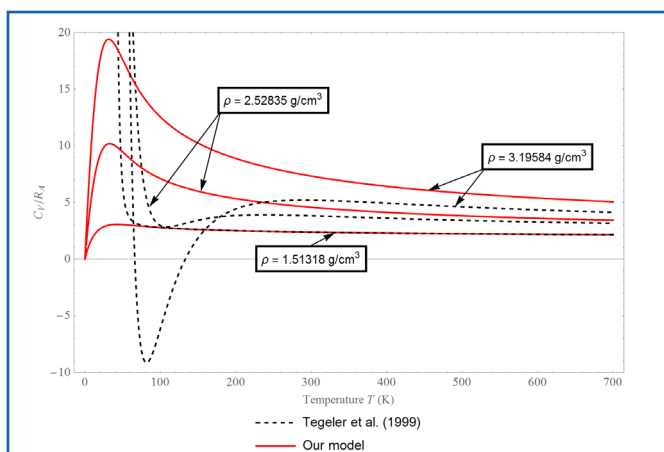


Figure 1: Isochoric heat capacity at very high densities from 0 K to 700 K. The plotted curves correspond to values calculated from our model (red curve) and from equation of state of Tegeler et al. (dashed curve). The latter are clearly unrealistic at low temperatures.

The widespread use of argon requires an accurate knowledge of its thermodynamic properties in the largest possible range of temperature and pressure. Numerous empirical equations of state can be found in the literature, but most of them cover only small parts of the fluid region.

The most recent wide-range empirical equation of state for argon was developed by Tegeler et al. (1999). The method is based on an empirical description of the Helmholtz free energy F as a function of density ρ and temperature T . However, as F is not accessible to direct measurements, a suitable mathematical structure and some fitted coefficients have to be determined from properties for which experimental data are available. In this model the expression of the residual part of F contains polynomial terms, gaussian terms and exponential terms which results in a total of 41 coefficients. This equation of state can describe experimental data for the fluid region in the temperature and pressure ranges:

$$83.8058 \text{ K} < T < 700 \text{ K}, \quad \text{and} \quad 0 \text{ MPa} < P < 1000 \text{ MPa}.$$

This equation of state has however many disadvantages, such as for example:

- The extrapolation of the equation for the isochoric heat capacity in regions of high or low densities and high or low temperatures is unrealistic.
- The model applies only for the pure fluid phases and cannot be simply modified to take into account particular properties inside the coexistence liquid-vapour region. Moreover, the model predicts negative values of C_v on some isotherms inside the coexistence liquid-vapour region.

In view to obtain a better description of the experimental thermodynamic data of argon in a much wider temperature and pressure range (up to 2300 K and 50 000 MPa - data from NIST, Ronchi, L'Air Liquide), a new equation of state has been developed. This equation is based on an empirical description of the isochoric heat capacity $C_v(\rho, T)$, and the thermodynamics quantities (internal energy, entropy, free energy,) are then obtained by combining integrations of functions involving $C_v(\rho, T)$. An important feature of our model is to predict the appearance of a maximum on the isochoric heat capacity C_v along isochors (Figure 1). Such a maximum of C_v along isochors has experimentally been observed in other fluids such as for example water.

The present modelling using mainly power laws is clearly more physical than using polynomials. It also allows to significantly reducing the number of terms and parameters. The number of coefficients for the description of F is only 26 (compared to 41), without losing much precision.

CONTACT

Frédéric Aitken

frederic.aitken@g2elab.grenoble-inp.fr

FURTHER READING

A New Equation of State for Argon Covering the Fluid Region for Temperatures From the Melting Line to 2300 K at Pressures up to 50 000 MPa

F. Aitken, N. Bonifaci, A. Denat and F. Volino

Submitted to Fluid Phase Equilibria.

Dielectric characterization of an experimental model of a silica/epoxy interface submitted to a hygrothermal environment

The adverse effects of moisture and temperature on the electrical properties of epoxy-silica composites have often been illustrated. The dielectric strength is affected, as shown by the large decreases of the breakdown strength. Phenomena occurring at the interfaces are mainly involved in this degradation. The existence of a water layer at the surface of silica is thermodynamically inevitable. The water is tight to the silica surfaces through chemical and physical adsorption. A better insight into the dielectric behavior of this water interphase is a step towards the understanding and modelling of the dielectric strength of these structures.

A macroscopic experimental model of a silica/epoxy interface has been designed and realized for dielectric investigations (Figure 2). It consisted in interdigitated electrodes deposited on a silica plaque and molded in epoxy resin. The sample was submitted to an artificial hygrothermal conditioning at a temperature of 80 °C and under a relative humidity of 80 %.

As shown in the Argand diagrams (Figure 1) - diagram consisting in the representation of $-Z''$ vs Z' where Z' and Z'' are respectively the real and imaginary parts of the impedance-, the dielectric behavior exhibit a sudden change after 7-8 days. In the first period, the sample fits a parallel RC model, with R decreasing as the water content increased with time – the resistance R corresponding to the value of Z' at low frequency when $Z''=0$. Then, the onset of a second line at the right hand of the half-circles at low frequency is observed.

The known coefficient of water diffusion in the resin at 80 °C supports the fact that this sudden change occurred when the diffused water reached the quartz/resin interface. In the second period, once the water has reached the interface, an important interfacial polarization was observed at the electrodes. An interphase is formed at the silica/epoxy interface. At low frequencies, increasing quantities of ionic water species have time to cross the 2 mm wide inter-electrode gap and gather close to the electrodes.

Comparison of the dielectric behavior of a pure resin, without any interface with silica, lead in similar conditions to a resistance drop of three decades under moisture effect, whereas the voltage drop is two decades larger when a water interphase is formed at the epoxy/silica interface. The resistance of the water interphase at stabilization can be deduced at about 500 kΩ, leading to a surface resistivity to $\rho_s = 80 \times 10^6 \Omega$. Starting from this result, an estimation of the thickness of the water layer at the silica/epoxy interface can be proposed.

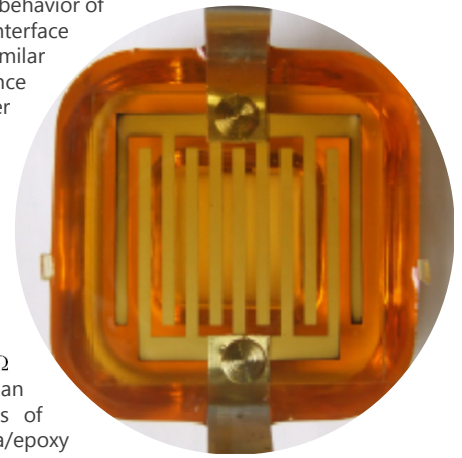


Figure 2 : Photograph of the sample with inter-digitated electrodes (electrodes 2 mm wide; gap distance 2 mm).

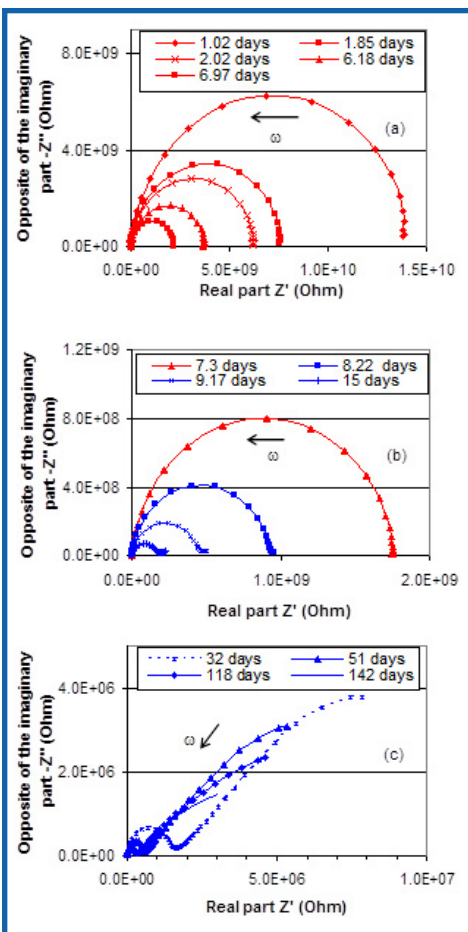


Figure 1 : Argand diagrams during the hygrothermal conditioning at 80 °C, 80 %R.H. Sample 1. Durations of conditioning: (a) 1 to 7 days; (b) 7 to 15 days; (c) 32 to 142 days

CONTACTS

Pascal Rain
 pascal.rain@g2elab.grenoble-inp.fr
 Ph.D Student
 Emilie Brun

FURTHER READING

Experimental model of a silica/epoxy interface submitted to a hygrothermal aging: a dielectric characterization
P. Rain, E. Brun, C. Guillermin and S. Rowe
 IEEE Trans. on Dielectrics and Elec. Insul., Vol. 19, Issue 1, pp. 343-351, February 2012.

EHD injection of water droplets of controlled micrometric size in dielectric liquids

We developed an injection system of electrically neutral droplets using Electrohydrodynamics (EHD) actuation technique. The method proposed consists in applying transient multi-stage electric pulses at a water meniscus hanging from a needle tip. Adaptations of geometry and applied voltage pulses allow extracting, from a single needle, droplet or droplet pairs in oil, with size ranging between 20 and 200 μm .

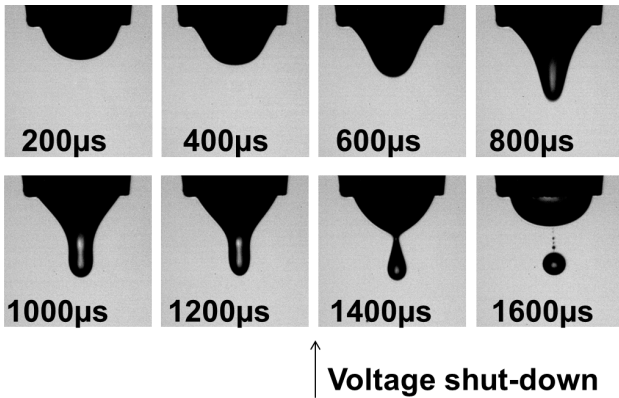


Figure 1: Visualization of water meniscus deformation and droplet ejection (diameter of needle tip: 1 mm)

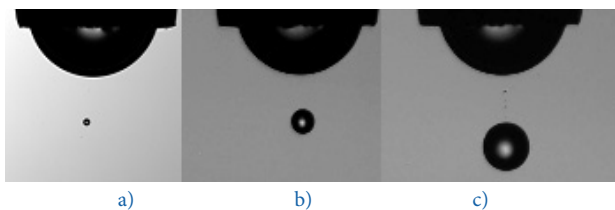


Figure 2: Different drop diameters obtained from the same needle by varying only the pulse amplitude
a) 20 μm , b) 80 μm , c) 170 μm

Electro-coalescence is used in the petroleum industry to separate water coproduced during extraction and desalting operation from the oil phase, if possible without using chemical demulsifiers. In-line flow compact electro-coalescers are designed to increase the mean size of water droplets by merging and therefore to reduce the time required for their sedimentation under gravity. Though, the control and increase of their efficiency remain particularly challenging as the numerous phenomena involved in electrocoalescence are far from being fully understood. To investigate critical coalescence conditions of water droplets in oil flows under the action of applied electric fields, drop pairs with diameter varying typically in the range 20-200 micrometres should be injected accurately in model oils to study by optical means, their relative motion, deformation and possible coalescence.

The developed on-demand EHD injection technique consists in the application of electric field pulses of calibrated energy to a meniscus of a conductive liquid immersed into a dielectric one. Due to the action of the induced electrostatic pressure, the interface, initially in equilibrium under the effects of gravity and capillary pressure, deforms and eventually becomes unstable, leading to the inertia-based ejection of one or more uncharged droplets.

Numerical simulations (figure 3) and experiments (figure 1) are associated to investigate the dynamics of menisci deformation and break-up. Development and analyses are performed through visualisations using high speed camera. The main influent parameters are: liquids density, interface tension and viscosity, initial meniscus shape at needle tip and applied multi-stage voltage pulse. Improvements of multi-stage pulse shape allow droplet injection from a single needle with the requested wide range of diameters (figure 2), a good reproducibility and stable ejection trajectories.

That study is performed in the framework of a collaborative research project ECIII: "Fundamental understanding of electrocoalescence in heavy crude oils", co-ordinated by SINTEF Energy Research - Norway.

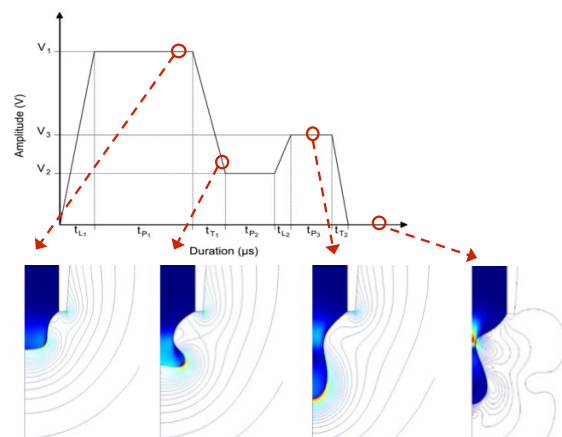


Figure 3: Shape of the multistage electric pulse $V(t)$ and simulation of water meniscus deformation under associated electrohydrodynamic forces. Diameter of needle tip is about 1 mm. Maximum water transient velocity –red color– is 1 m/s. (Comsol multiphysic™)

CONTACTS

Jean-Luc Reboud
 jean-luc.reboud@g2elab.grenoble-inp.fr
 Ph.D Student
 Jonathan Raisin

FURTHER READING

A novel actuation technique for the on-demand injection of charge free conducting droplets in a viscous dielectric liquid
 J. Raisin, P. Atten, J.L. Reboud
 Exp. in Fluids, Vol. 54, Issue 3, March 2013.

Infra-Red calorimeter applied to electrical engineering: a new calorimetric device based on thermal radiation for measuring losses in electrical components

Most calorimetric methods currently used have a number of limitations both in their power range, frequency, voltage or operating temperature, as well as in the geometry of the power component to be tested. To overcome these limitations, we have designed and implemented a new calorimetric device based on heat radiation. Thus, we have surpassed the inconvenience commonly encountered in current calorimeters. This calorimeter was constructed using an analytical model of the heat exchange between the different elements.



We have designed and developed a new device of calorimetry for characterizing the power losses in electric components. In this calorimeter, the heat exchange between the component and the measuring cell occurs by thermal radiation. This principle eliminates the constraint of component geometry. As it operates in a temperature range of 200 to 400K, the calorimeter allows to measure the losses as a function of the controlled temperature. The electrical component may be supplied by a voltage of arbitrary waveform with magnitudes up to 3 kV. Analysis of results obtained on components has shown that measurement error was less than 5% for a range of dissipation power ranging from mW to W. This device has been developed with the support of the service of scientific instrumentation of Neel Institute (SERAS). This calorimeter is now used by SIREPE SAS, a startup specialized in energy conversion systems. Thermal losses of the component under study are derived by the differential method. The power P_0 is measured when the voltage is off and the power P_1 is measured when the voltage is on. The losses P are thus deduced: $P = P_0 - P_1 + \Delta P$, with an error ΔP .

ΔP represents the error of measurement due to a physical variation of powers exchanged between the measuring cell and the other parts of the device (thermostat cryogenic, thermal shield and vacuum enclosure) between the two instants of P_0 and P_1 .

CONTACTS

Olivier Gallot-lavallee

olivier.gallot-lavallee@g2elab.grenoble-inp.fr

Frédéric Aitken

frederic.aitken@g2elab.grenoble-inp.fr

Ph.D Student

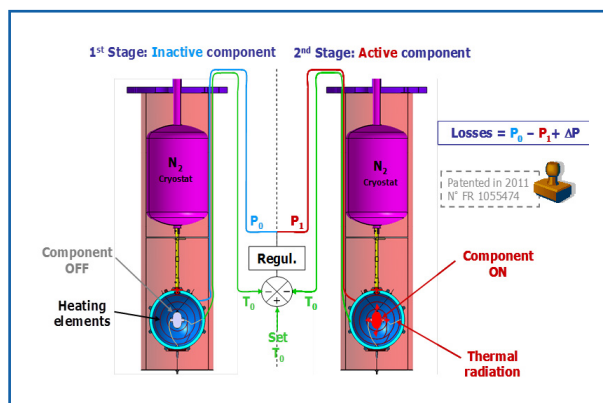
Elysée Obame

FURTHER READING

Application de la calorimétrie I.R. à la mesure des pertes dans les systèmes et composants de puissance
E. Obame, C. Rizet, S. Vighetti, O. Gallot-Lavallée, F. Aitken
sciencesconf.org/sge2014:29931.

Système calorimétrique et procédé pour mesurer les pertes de puissance dans un composant électrique

O. Gallot-Lavallee, F. Aitken, E. Obame
N° Brevet FR2962539, N° Enregistrement FR20100055474, Paris, France, Enregistré le 06-07-2010, Publié le 13-01-2012.



Deviations to the Paschen law at distances down to 100 nm: from a gas discharge to a metallic plasma

Measurements of breakdown voltages in Air and Nitrogen are carried out in very short gaps down to 100 nm thanks to the development of a specific instrumentation. Below 1 μm , breakdown voltages considerably deviate from the classical Paschen law, with a nearly constant breakdown field about 350 V/ μm . In these conditions, spectroscopic measurements show that the breakdown mechanism changes from a gas discharge to a metallic plasma.

The electrical breakdown of gases is described over a large range of pressure and distances by the Paschen law, based on the well-established model involving charge multiplication by electron avalanches. However, with very short gap distances (typically less than 4 μm at atmospheric pressure), measurements deviate from the Paschen law: breakdown voltages become lower than predicted ones. Although several studies of breakdown in small gaps were already carried out, a large scatter of data is observed, and no definitive consensus on the mechanisms has emerged. Breakdown in very short gaps addresses various application domains. In integrated MEMS relays, the distance between activation electrodes and between contacts is below 1 μm . Breakdown phenomena at the nanometer scale are thus very important for the design and reliability of these systems. Concerning ageing processes of solid insulating materials, the scenario frequently proposed to explain the final transition to breakdown involves the appearance of "partial discharges" within cavities of sub-micrometer size.

A key point: the transition from a gas discharge to a metallic plasma at very short gaps < 1 μm
Measurements of breakdown voltage in very small gaps coupled to a spectroscopic analysis of the emitted light were carried out for the

first time in the framework of a cooperation with CEA – LETI laboratory of Grenoble, specialized in integration technologies. Measurements were carried out both with real MEMS switches, and with a specific electrode arrangement allowing us to adjust the gap distance down to 100 nm with an accuracy of 30 nm. Spectroscopic measurements were especially challenging due to the very small amount of emitted light, and required the accumulation of a large number of spectra.

Figure 1a shows the large deviation to the Paschen law observed for gaps below 1 μm . At 100 nm distance, the onset of discharges at voltage as low as 30 V is quite far from the classical Paschen law, that predicts no discharges in air below 350 V. The spectroscopic analysis provides an insight into the discharge mechanism involved. At voltage < 50 V (distance < 200 nm) spectra are characteristic for a metallic plasma induced by the vaporization of electrodes (figure 1b), and do not show any more the usual features of a gas discharge. These results provide useful knowledge for the design and testing of MEMS switches, and also for a better understanding of degradation processes of dielectrics. Further work will include the influence of gas nature and pressure on these measurements.

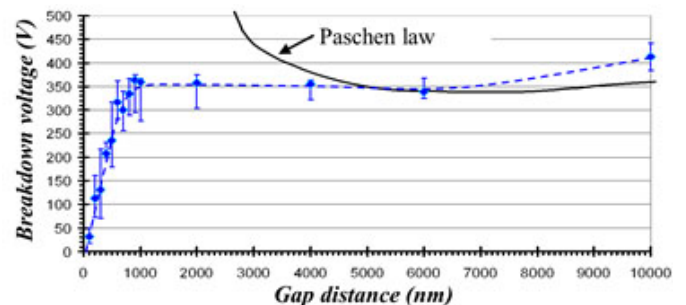


Figure 1a: Deviation to the Paschen law at short gaps

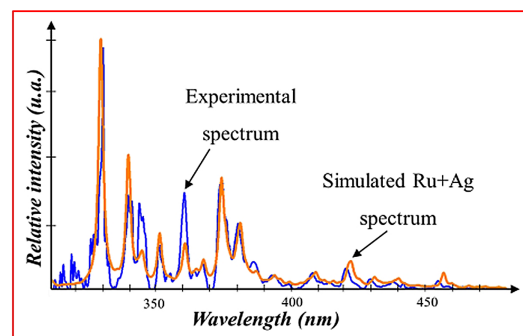


Figure 1b: spectrum recorded at 50 V (air, atmospheric pressure, Ruthenium/Silver electrodes).

CONTACTS

Olivier LESAIN

olivier.lesaint@g2elab.grenoble-inp.fr

Nelly Bonifaci

nelly.bonifaci@g2elab.grenoble-inp.fr

Ph.D Student

Alexis Peschot

FURTHER READING

Spectroscopic analysis of material transfer phenomena in MEMS switches

A. Peschot et al.

IEEE IRPS, ME.3.1-ME.3.5, (2013)

Deviations from the Paschen's law at short gap distances from 100 nm to 10 μm in air and nitrogen

A. Peschot, N. Bonifaci, O. Lesaint, C. Valadares, C. Poulain

Appl. Phys. Lett. 105, 123109 (2014)

“Dark” currents in pressurized air and SF6 under HVDC: the crucial role of adsorbed water

High electric fields above 10 kV/mm can be applied to pressurized gases such as Sulphur Hexafluoride (SF6) without breakdown. High sensitivity current measurements with a sub-picoampere resolution under direct high voltage (HVDC), allow us to evidence “dark” currents of unexpected amplitudes flowing through pressurized air and SF6 under high electric field. The presence of water adsorbed on electrode surfaces has a very large impact on these currents.

Pressurized gases such as SF6 are used for the electrical insulation of various high voltages systems, including GIS (Gas Insulated Switchgear) and GITL (Gas Insulated Transmission Line). Pressurized gases are characterized by excellent dielectric properties: a high breakdown field and a very low “electrical conductivity”. Under ac high voltage, the extremely low conduction current able to flow across the gas has no practical influence. In HVDC systems, when gases are associated with insulating solids of very high resistivity, even very small currents crossing the gas may have an impact on the system reliability. Charges coming from the gas may accumulate on solid surfaces over long periods of time, and lead to the building of a surface charge density large enough to modify the initial field distribution. Numerous detailed studies were previously carried out about high field conduction mechanisms in vacuum, but not in pressurized gases.

A key point evidenced at G2Elab: the crucial influence of adsorbed water on electrodes

Measurements of very small currents in pressurized gases under high HVDC fields have been carried out in the framework of an international cooperation with Siemens Company. The development of a specific high voltage instrumentation (figure 1), allows measurements of currents in pressurized Air and SF6 in various conditions of gas pressure and relative humidity, with a resolution down to 100 femto-amperes at voltage up to 350 kV.

In conditions relevant of practical industrial systems, unexpected large currents are measured. These currents far exceed theoretical values considered in most previous simulations, developed by considering that electrical charges appear only due to the “natural” gas ionization

(induced by cosmic rays). Natural gas ionization is able to provide electron/ion pairs at a rate about $5\text{-}30\text{ cm}^{-3}\cdot\text{s}^{-1}$ depending on gas pressure, and should induce current densities about $5\text{ }10^{-18}\text{ A/cm}^2$ in typical conditions. Measurements at fields above 2 kV/mm indicate considerably larger values ($> 5\text{ }10^{-11}\text{ A/cm}^2$, figure 2), and show the influence of charge injection from electrodes at high field.

A very important new parameter evidenced in these measurements concerns the influence of water adsorbed on electrodes. Since in practical applications of SF6 water cannot be totally removed, this parameter is thus of great importance under HVDC. Further experiments are currently done to better understand the complex influences of the gas relative humidity, temperature, and electrode surface processing on dark currents



Figure 1: HVDC 350 kV test cell for the measurement of dark currents through pressurized gases.

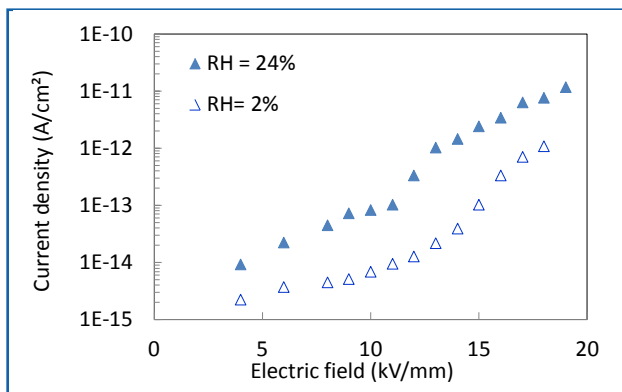


Figure 2: Dark current density in SF6 versus electric field, with two values of the gas relative humidity RH (0.6 MPa, 10 mm gap distance)

CONTACTS

Olivier Lesaint

olivier.lesaint@g2elab.grenoble-inp.fr

Ph.D Student

Laetitia Zavattoni

FURTHER READING

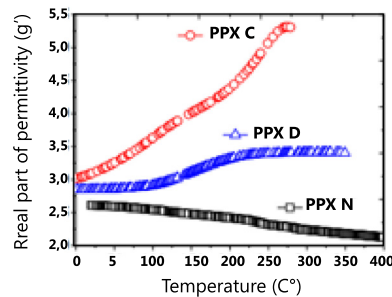
Dark Current Measurements in Pressurized Air, N2, and SF6

L. Zavattoni, O. Lesaint, O. Gallot-Lavallée
Conf. on Elec. Insul. and Diel. Phen., CEIDP, IEEE, Shenzhen, Chine, pp. 659-662, October 20-23, 2013

Physical and electric properties of various parylene families

Parylene is a polymer which settles in thin layer by chemical vapor deposition (CVD). Its hydrophobic properties, its conformability, its strong barrier to humidity and gases, its transparency, its good dielectric performances, its wide range of temperature use, its biocompatibility make this inescapable polymer in applications always more numerous and diversified. Paradoxically, its (di)electric properties in connection with its physico-chemical properties have been poorly studied. The aim of our study consisted in particular in making this link through several families of parylene.

Dielectric constant (@1kHz) for three families of parylene



The aim of this study was to analyze in depth the dielectric properties and the conductivity of six families of parylene in relation with their structural properties (degree of crystallinity, rugosity...) but also an analysis of the changes operated on these materials following the conditions of process during the deposition of these polymers (substrate temperature, post-annealing...). Beyond the scientific interpretations, these works constitute an important database on these materials at the same time for the researchers and the industrialists incorporating these polymers for their applications. So, the originality of this work becomes famous through the numerous results and the publications produced (see below).

Families of parylene	Chemical formulation	Chemical structure
Parylene N (PPX N)	(C ₈ H ₈)	
Parylene C (PPX C)	(C ₈ H ₇ Cl)	
Parylene D (PPX D)	(C ₈ H ₆ Cl ₂)	
Parylene F or Dix-F	(C ₈ H ₆ F ₂)	
Parylene AF-4 or parylene HT	(C ₈ H ₄ F ₄)	
Parylene VT-4	(C ₈ H ₄ F ₄)	

Chemical structure of different families of parylene

The originality is the number of original works published on this topic over a short period

1. A. Kahouli, A. Sylvestre, L. Ortega, F. Jomni, B. Yangui, M. Maillard, B. Berge, J.C. Robert, J. Legrand 'Structural and dielectric study of parylene C thin films', Applied Physics Letters, 94(15), 152901, 2009.
2. A. Kahouli, F. Jomni, A. Sylvestre, B. Yangui, J. Legrand 'I-t, J-1/T and J-E characteristics for the understanding of the main mechanism of electric conduction and the determination of the glass transition temperature of parylene C thin films', Journal of Physics D: Applied Physics, 44, 505302 (6 pp.), 2011.
3. A. Kahouli, A. Sylvestre, F. Jomni, B. Yangui, J. Legrand 'Ac-conductivity and dielectric relaxations above glass transition temperature for parylene-C thin films', Applied Physics A, 106, pp. 909-913, 2012.
4. A. Kahouli, A. Sylvestre, F. Jomni, E. André, J.-L. Garden, B. Yangui, B. Berge, J. Legrand 'Dielectric properties of parylene AF4 as low-k material for microelectronic applications', Thin Solid Films, 520, 7, pp. 2493-2497, 2012.
5. A. Kahouli, A. Sylvestre, F. Jomni, B. Yangui, J. Legrand 'Experimental and theoretical study of AC electrical conduction mechanisms of semicrystalline parylene C thin films', The Journal of Physical Chemistry A, 116(3), pp. 1051-1058, 2012.
6. A. Kahouli, A. Sylvestre, S. Pairis, J.F. Lathier, 'Effect of ClH aromatic substitution on structural and dielectric properties of poly(p-xylylene)', Polymer, 53, pp. 3001-07, 2012.
7. A. Kahouli, E. André, A. Sylvestre, S. Pairis, F. Jomni, B. Yangui, J.-L. Garden: 'Structure and dielectric study of poly(□, □ difluoro-p-xylylene) thin films: highlight of the substrate temperature effect', Chemical Vapor Deposition, 18, issue 4-6, pp. 147-150, 2012.
8. A. Kahouli, A. Sylvestre, S. Pairis, J.-L. Garden, E. André, F. Jomni, B. Yangui 'Effect of O₂, Ar/H₂ and CF₄ plasma treatments on the structural and dielectric properties of parylene-C thin films', Journal of Physics D: Applied Physics, 45, 215306 (7 pp), 2012.
9. A. Kahouli, L. Wei, A. Lakhtakia, A. Sylvestre 'Low-frequency dielectric functions of dense and chevronic thin films of parylene C', Materials Letters, 95, 63-66, 2013.
10. A. Kahouli, A. Sylvestre, J.F. Lathier 'Performance improvements of the hydrophobic and the dielectric properties of parylene C', Journal of Applied Physics, 114, 154111 (7 pp.), 2013.
11. A. Kahouli, A. Sylvestre, J.F. Lathier, L. Lutsen, S. Pairis, E. André, J.-L. Garden 'Structural and dielectric properties of parylene-VT4 thin films', Materials Chemistry and Physics, 143, 908-914, 2014.
12. A. Kahouli, A. Sylvestre, J.F. Lathier, L. Lutsen, S. Pairis, E. André, J.-L. Garden 'Evaluation of Activation Parameters of Molecular Mobility of Parylene C Using Differential Scanning Calorimetry, Dielectric Spectroscopy, and Thermally Stimulated Depolarization Currents', The Journal of Physical Chemistry A, 118(8), 1320-1330, 2014.

CONTACTS

Alain Sylvestre

alain.sylvestre@g2elab.grenoble-inp.fr

Ph.D Student

Abdelkader Kahouli

FURTHER READING

A. Kahouli

Etude des propriétés physico-chimiques et diélectriques du parylène C en couche mince,

Thèse de l'Université de Grenoble et de l'Université de Carthage, soutenue le 1 Avril 2011

G2Elab

Grenoble Electrical Engineering

Site : Domaine Universitaire
ENSE³
BP 46
38402 St Martin d'Hères
Cedex, France
Tél. +33 (0)4 76 82 62 99
Fax +33 (0)4 76 82 63 00

Site : Polygone Scientifique
CNRS
BP 166
38042 Grenoble
Cedex 9, France
Tél. +33 (0)4 76 88 78 83
Fax +33 (0)4 76 88 79 45

www.G2Elab.grenoble-inp.fr

